AGU
ADVANCING
EARTH AND
SPACE SCIENCE

# Geophysical Research Letters

## Open Ocean Particle Flux Variability From Surface to Seafloor

**B. B. Cael[1]** [ID], **Kelsey Bisson[2]** [ID], **Maureen Conte[3,4]**, **Manon T. Duret[5]** [ID], **Christopher L. Follett[6]** [ID], **Stephanie A. Henson[1]** [ID], **Makio C. Honda[7]**, **Morten H. Iversen[8,9]** [ID], **David M. Karl[10]** [ID], **Richard S. Lampitt[1]**, **Colleen B. Mouw[11]** [ID], **Frank Muller-Karger[12]** [ID], **Corinne A. Pebody[1]**, **Kenneth L. Smith Jr.[13]**, and **David Talmy[14]**

[1]National Oceanography Centre, Southampton, UK, [2]Oregon State University, Corvallis, OR, USA, [3]Bermuda Institute of Ocean Sciences, St Georges, Bermuda, [4]Marine Biological Laboratory, Woods Hole, MA, USA, [5]University of Southampton, Southampton, UK, [6]Massachusetts Institute of Technology, Cambridge, MA, USA, [7]Japan Agency for Marine-Earth Science and Technology, Yokosuka, Kanagawa, Japan, [8]Alfred Wegener Institute, Bremerhaven, Germany, [9]MARUM and University of Bremen, Bremen, Germany, [10]University of Hawai'i at Manoa, Honolulu, HI, USA, [11]University of Rhode Island, Narragansett, RI, USA, [12]University of South Florida, St. Petersburg, FL, USA, [13]Monterey Bay Aquarium Research Institute, Moss Landing, CA, USA, [14]University of Tennessee-Knoxville, Knoxville, TN, USA

**Abstract** The sinking of carbon fixed via net primary production (NPP) into the ocean interior is an important part of marine biogeochemical cycles. NPP measurements follow a log-normal probability distribution, meaning NPP variations can be simply described by two parameters despite NPP's complexity. By analyzing a global database of open ocean particle fluxes, we show that this log-normal probability distribution propagates into the variations of near-seafloor fluxes of particulate organic carbon (POC), calcium carbonate, and opal. Deep-sea particle fluxes at subtropical and temperate time-series sites follow the same log-normal probability distribution, strongly suggesting the log-normal description is robust and applies on multiple scales. This log-normality implies that 29% of the highest measurements are responsible for 71% of the total near-seafloor POC flux. We discuss possible causes for the dampening of variability from NPP to deep-sea POC flux, and present an updated relationship predicting POC flux from mineral flux and depth.

**Plain Language Summary** Understanding the oceanic cycles of carbon and other elements important for life, as well as how ocean life influences the Earth's climate, we must understand how the carbon fixed by phytoplankton during photosynthesis is consumed and redistributed throughout the ocean. How much carbon is fixed at a given place and time varies substantially based on a number of factors; out of this complexity, however, emerges a simple description in terms of a probability distribution: The log-normal. Here, we show that this log-normal description propagates all the way from the upper ocean to the seafloor. We find that this log-normal description is robust, applying both to the global open ocean and to individual locations. Our results help resolve the long-standing question of to what extent seafloor communities rely on a steady supply of energy versus large pulses. Our results also shed light on the known connection between the vertical transport of organic carbon and those of calcium carbonate and opal. We also find that variability in primary production is dampened on its way to the seafloor in a consistent fashion.

## 1. Introduction

Ocean biogeochemical cycles have much to do with vertical transport of carbon and other elements via particle sinking and other processes (Boyd et al., 2019). Net primary production (NPP) by phytoplankton largely controls how much carbon is available to the rest of the ecosystem (Osmond, 1989); most of this sustains the heterotrophic communities living in the euphotic zone, but a fraction is transported to deeper depths. This fraction is comparably small in the context of the carbon cycle (Muller-Karger et al., 2005) but results in a vertical flux that redistributes carbon and other elements from the surface all the way to the seafloor, connecting the ocean as a global ecosystem while also storing thousands of petagrams of carbon in deep waters for climatically relevant timescales (Ito & Follows, 2005). Quantitative understanding of this flux remains limited, however, not only because measurements of sinking particle flux are challenging and

expensive (and commensurately sparse), but also because these measurements are highly variable (Buesseler & Boyd, 2009; Buesseler et al., 2007; Cael et al., 2018; Mouw et al., 2016). Estimates of the global export of organic carbon out of the upper ocean vary by more than a factor of three (Bisson et al., 2018; Boyd & Trull, 2007; Henson et al., 2011), with fluxes to the deep ocean being less constrained.

One long-standing question is whether the majority of mass and energy is delivered as a steady background level or from rare deposition events (Rokop, 1974; Smith et al., 2014). Addressing this question is not straightforward. Although NPP and deep-sea flux are undoubtedly linked, predicting flux from NPP is challenging on a point-by-point basis because such observations decouple over space and time and because flux-generating processes are not directly a function of primary production (Buesseler, 1998; Cael et al., 2018; Plattner et al., 2005; Footnote 1 in the supporting information). Yet, quantitative understanding of the vertical fluxes of carbon and other elements requires characterizing their variability. Capturing the probability distribution of deep-sea flux allows one to quantify how episodic it is, and can provide a simple yet comprehensive way to describe the flux of carbon, its variability, and its relationship with other fluxes. Cael et al. (2018) showed that NPP is robustly well-characterized by a log-normal probability distribution, meaning its extensive variability can be described by just two parameters (the log-mean $\mu$ and the log-standard deviation $\sigma$; Footnote 2 in the supporting information). Similarly as for many other natural phenomena (Limpert et al., 2001), this distribution is thought to emerge because NPP is the product of both structured (e.g., average nutrient supply to the surface) and stochastic (e.g., turbulent mixing) processes. POC export out of the upper ocean also follows a log-normal distribution, though the statistical power behind this statement is limited by sample size (Cael et al., 2018).

Here, we show that the log-normal character of NPP propagates down to deep-sea measurements of POC flux, further demonstrating that the log-normal is a robust feature of variations in ocean carbon fluxes. We show that log-normality holds not only for a collection of global open ocean measurements, but also for measurements from individual time-series, indicating its consistency across scales. Furthermore, log-normality holds not only for POC but also for calcium carbonate and opal, which are thought to play an important role in the vertical transport of POC (Armstrong et al., 2001; Wiedmann et al., 2020). So-called "ballast" minerals are known to be strong predictors of POC flux, although it is still disputed whether this effect is mechanistic or coincidental (Footnote 3 in the supporting information; Passow & De La Rocha, 2006). Our results suggest (1) an updated global relationship between mineral and POC fluxes, (2) that POC deposition to the seafloor, and hence supplied to benthic communities, is episodic, but not enough so to meet the 80/20 Pareto principle benchmark for a heavily imbalanced phenomenon in other contexts (Sanders, 1987), and (3) that marine heterotrophs may dampen variability in NPP by consuming a higher fraction of NPP when NPP is larger (Footnote 4 in the supporting information).

## 2. Global Open Ocean Fluxes

The POC flux through the water column at a particular location and time follows a flux profile $\mathcal{F}(z)$ (mg C m$^{-2}$ d$^{-1}$) that attenuates with depth (Suess, 1980). This implies that an initial flux from some reference depth $z_o$, is attenuated through the water column by an "attenuation factor" $a$ so that the flux making it to the seafloor $\mathcal{F}_s = a\mathcal{F}(z_o)$. We may further define an export efficiency $ef$ (Eppley & Peterson, 1979) as the ratio between POC flux and NPP such that $\mathcal{F}_s = a\mathcal{F}(z_o) = a \times ef \times$ NPP. Since the log-normal emerges from the product of multiple random variables, one might expect that if POC export $\mathcal{F}(z_o)$ or NPP are log-normally distributed (Cael et al., 2018), we should expect $\mathcal{F}_s$ to be log-normally distributed as well, as one is just multiplying by more terms. Log-normality would propagate through depth as long as $a$ (or $a \times ef$) scales with $\mathcal{F}(z_o)$ (or NPP) in some way, is roughly constant, or randomly varying according to some well-behaved probability distribution (i.e., a probability distribution with finite variance). Log-normality would not extend to $\mathcal{F}_s$ if, for instance, $a \times ef$ had a more complex dependence on NPP such as if $a \times ef$ sharply increases above a threshold NPP value, or $a \times ef \approx 0$ for large NPP values (SI). Given that attenuation and export efficiency are both quite variable (Cael & Follows, 2016; Henson et al., 2012), we hypothesize that this log-normality of NPP should propagate all the way to the seafloor flux $\mathcal{F}_s$ (Footnote 5 in the supporting information).
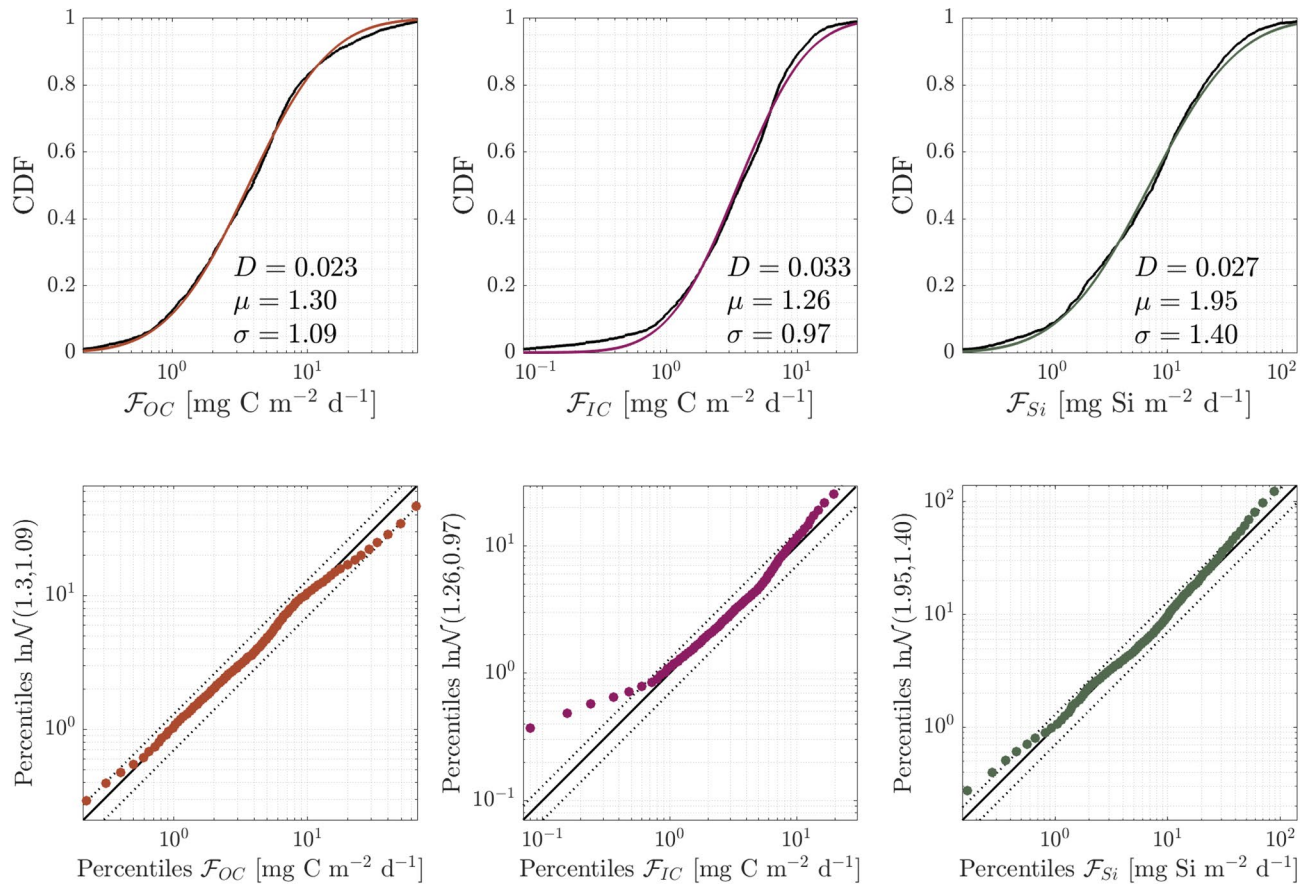
**Figure 1.** Top: Empirical cumulative distribution functions for bathypelagic near-seafloor particulate organic carbon, calcium carbonate, and opal fluxes (black lines) from Mouw et al. (2016), with fitted log-normal distributions overlaid (colored lines). $D$ is the Kolmogorov-Smirnov statistic; $(\mu, \sigma)$ are the log-mean and log-standard deviation of the log-normal distributions corresponding to the colored lines. Bottom: Percentiles of the empirical ($x$-axis) versus log-normal ($y$-axis) distributions from the top panels. Solid black line is the 1:1 line and the dotted lines represent a standard 30% measurement error (Buesseler et al., 2000, 2007; Cael & Bisson, 2018; Stanley et al., 2004).

This hypothesis is readily testable on the global scale thanks to the comprehensive database of particle flux measurements assembled by Mouw et al. (2016). We extracted from this database all of the measurements which were made at or below 1 km depth, and within 1 km of the seafloor, totaling 3,337 sediment trap measurements of bathypelagic POC flux ($\mathcal{F}_{OC}$, [mg C m$^{-2}$ d$^{-1}$]), which we consider sufficiently near the seafloor to make inferences about the statistics of seafloor fluxes (Footnote 6 in the supporting information). As $\mathcal{F}_{OC}$ is generally tightly correlated with mineral fluxes (Armstrong et al., 2001; Francois et al., 2002; Henson et al., 2012; Klaas & Archer, 2002), we apply the same selection criteria for fluxes of calcium carbonate (calcite and aragonite, $\mathcal{F}_{IC}$) and opal ($\mathcal{F}_{Si}$), resulting in 2,968 $\mathcal{F}_{IC}$ measurements and 2,821 $\mathcal{F}_{Si}$ measurements (we also corroborate these correlations here). While these data are spatially biased, for example, toward under-representing polar or shelf regions (§Episodicity) we take them to be a representative random sample of near-seafloor bathypelagic particle fluxes for the global open ocean. We test the log-normality of these data using the standard Kolmogorov-Smirnov cumulative distribution function (CDF) metric $D = \max_{\mathcal{F}} |P_1(\mathcal{F}) - P_2(\mathcal{F})|$, where $P_1$ and $P_2$ are the CDFs of $\mathcal{F}$; here we are comparing the empirical CDF of the data itself with a hypothesized log-normal distribution's CDF. As in Cael et al. (2018) we fit a log-normal distribution to each of these three measurement sets ($\mathcal{F}_{OC}$, $\mathcal{F}_{IC}$, and $\mathcal{F}_{Si}$), estimating the log-moments by minimizing this fitting statistic. We use $D$ because it is the simplest such statistic (Stephens, 1974); other choices yielded the same results.

We find that all three of these measurements are well-described as log-normal, with $D$ values well below the thresholds to reject this hypothesis at the 5% significance level (Stephens, 1974). Figure 1 shows the

hypothesized and empirical CDFs as well as the percentile-percentile plots which indicate that the log-normal approximation predicts the percentiles of all three measurement fluxes' distributions within a standard measurement error of 30% (Buesseler et al., 2000, 2007; Cael & Bisson, 2018; Stanley et al., 2004; Footnote 7 in the supporting information) except for the smallest percentiles of the mineral fluxes where the absolute deviations are still small ($<0.3$ mg C m$^{-2}$ d$^{-1}$). Altogether there is clear statistical evidence that globally all of these fluxes are log-normally distributed, and errors introduced by this approximation are either within standard measurement error and/or very small.

## 3. Time-Series Fluxes

Is this observed log-normality just a coincident feature of where and when these measurements have historically been taken, or of large-scale biogeochemical cycles? Or is it a robust feature of ocean particle fluxes? The argument presented in the previous section is, in principle, equally applicable on smaller scales. A stricter test of our hypothesis is whether it holds for individual locations, that is, data from time-series stations; encouragingly, these fluxes are known to be episodic (Karl et al., 2012; Smith et al., 2018), consistent with log-normality.

We apply the log-normal fitting procedure from the previous section to data from six deep-sea sediment trap time-series locations:

- A Long-term Oligotrophic Habitat Assessment (ALOHA) in the North Pacific Subtropical Gyre, a system which despite being perennially oligotrophic exhibits surprising variability in community structure and export (Follett et al., 2018; Karl et al., 2012) and even interannual variations in nutrient limitation (Letelier et al., 2019)
- The Carbon Retention in a Colored Ocean (CARIACO) time-series in the Caribbean Sea, a near-coastal site also affected by terrestrial processes (Muller-Karger et al., 2019)
- Station K2 in the subarctic Northwest Pacific, a mesotrophic system with important dust-borne inputs of the limiting micronutrient iron (Honda, 2020; Lam & Bishop, 2008)
- Station M in the Northeast Pacific, a site within the California Current, an upwelling system that is productive and highly variable not only seasonally but also on short timescales as well as interannually (Smith et al., 2018)
- The Oceanic Flux Program (OFP) time-series in the Sargasso Sea (Conte & Weber, 2014; Conte et al., 2001, 2003, 2019), an oligotrophic system with significant blooms and interannual variability (Lomas et al., 2013; Steinberg et al., 2001)
- The Porcupine Abyssal Plain (PAP) time-series in the North Atlantic Ocean, a temperate system exhibiting spring blooms, but also strong influences by turbulent ocean features as well as climatic drivers (Lampitt et al., 2010)

Further details about each time-series can be found in the above references. Collectively, the near-seafloor sediment traps from these time-series span measurements from a diversity of ocean settings; for example, eutrophic/oligotrophic environments, nutrient and oxygen status, or seafloor depth (Lampitt et al., 2010). The trap depths are 4,000 m (ALOHA), 1,210 m (CARIACO), 4,810 m (K2), 3,400 m (M), 3,200 m (OFP), and 3,000 m (PAP). We obtained 452/325/305 measurements from Station ALOHA of $\mathcal{F}_{OC/IC/Si}$, 665/665/400 measurements from OFP of $\mathcal{F}_{OC/IC/Si}$, 232/240/240 measurements from Station K2 of $\mathcal{F}_{OC/IC/Si}$, 723/557 measurements from Station M of $\mathcal{F}_{OC/IC}$, 294/166 measurements from PAP of $\mathcal{F}_{OC/IC}$, and 371/366/345 measurements from CARIACO of $\mathcal{F}_{OC/IC/Si}$. Some of these sample sizes are somewhat small to rigorously test for log-normality for individual data sets, but collectively they can demonstrate the robustness (or lack thereof) of the log-normal distribution on different spatial scales and at different locations; our conclusions are not sensitive to the inclusion/exclusion of any particular time-series.

Figure 2 shows the results of fitting the individual time-series' data. As for the global data sets, the deviations between the empirical and theoretical distributions are not statistically significant, and the percentiles tend to stay within standard measurement error and/or represent small absolute deviations in the low tails, one exception being the very highest percentiles of the PAP $\mathcal{F}_{IC}$ distribution, which is likely attributable to this having the smallest sample size ($N = 166$), and therefore these percentiles being very sensitive to the exact values of the largest two to three measurements. The other exception is the highest few percentiles
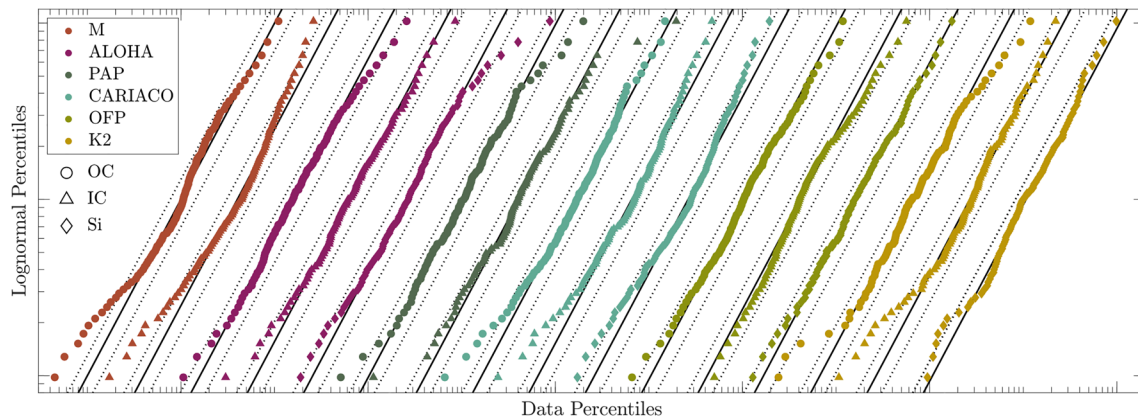
**Figure 2.** As in the bottom row of Figure 1, but for the individual time-series' data. Color indicates station and shape indicates measurement. Solid black line is the 1:1 line and the dotted lines represent a standard 30% measurement error (Buesseler et al., 2000, 2007; Cael & Bisson, 2018; Stanley et al., 2004).

of the ALOHA $\mathcal{F}_{Si}$ distribution, which are more intriguing and suggest that the processes governing the diatom-diazotroph-association-dominated summer export pulse (Follett et al., 2018; Karl et al., 2012) in the North Pacific Subtropical Gyre may be capable of "breaking" this distributional description of particle flux and generate deep-sea fluxes substantially larger than would be otherwise predicted. Outside of these anomalously large opal fluxes, however, these time-series data corroborate the robustness of the log-normal description of deep-sea particle fluxes.

## 4. Mineral Scaling

As mineral fluxes and POC fluxes are both log-normally distributed, this implies that a scaling relationship is a more appropriate way to relate the two fluxes than multi-linear regression (Armstrong et al., 2001; Francois et al., 2002; Henson et al., 2011; Klaas & Archer, 2002). The global $\mathcal{F}_{OC/IC/Si}$ measurements present an opportunity to update the classic multi-linear regression equations for mineral flux, though it is important that variation in depth is also accounted for, as depth-normalization can introduce substantial uncertainty (Cael & Bisson, 2018; Olli, 2015). For these regressions, we restrict the global measurements of Mouw et al. (2016) shown in Figure 1 to the 2,798 coincident measurements of all three fluxes and fit the function:

$$\mathcal{F}_{OC} = \kappa \left( \mathcal{F}_{IC} + \beta \mathcal{F}_{Si} \right)^{\gamma} \left( \frac{z}{3500} \right)^{-b}$$

where $\kappa$ and $\gamma$ are the parameters of a standard scaling relationship, that is, $y = \kappa x^{\gamma}$, $b$ is the standard "Martin curve" exponent, and $\beta$ then represents the ratio of organic carbon association per unit mass for opal versus calcium carbonate, which some may interpret as a ballast effect. In effect, this equation is asking how $\mathcal{F}_{OC}$, normalized (Footnote 2 in the supporting information) to a uniform depth of 3,500 m by a power law (Martin et al., 1987), scales with mineral flux. We also assume multiplicative (i.e., % rather than absolute) errors, consistent with these variables scaling with one another and being log-normally distributed. As both $\mathcal{F}_{OC}$ and $\mathcal{F}_{IC} + \beta \mathcal{F}_{Si}$ have errors, a model II regression is necessary; we use major axis regression, but our results are insensitive to this choice. We identify the $(\beta, b)$ pair that yields the best fit regression between $(z / 3500)^{b} \mathcal{F}_{OC}$ and $\mathcal{F}_{IC} + \beta \mathcal{F}_{Si}$, and repeat this procedure 1,000 times with bootstrap resampling to estimate uncertainty in all of the parameters $(\kappa, \beta, \gamma, b)$.

Figure 3 shows the results of fitting this model; we see that a scaling relationship is an effective description of this relationship ($r^2 = 0.66$ for the dashed line in Figure 3; Footnote 9 in the supporting information), with depth-normalized POC flux scaling with mineral flux to the $\gamma = 1.06 \pm 0.01$. This exponent is slightly – but statistically significantly – larger than 1, corresponding to a slightly systematically increasing POC/mineral ratio with increasing mineral flux. Furthermore, we find $\beta = 0.26 \pm 0.01$ suggesting that roughly four times as much organic carbon is associated with calcium carbonate per unit mass relative to opal. Interestingly, we find a slightly high (Footnote 10 in the supporting information) $b$ value of $1.16 \pm 0.03$.
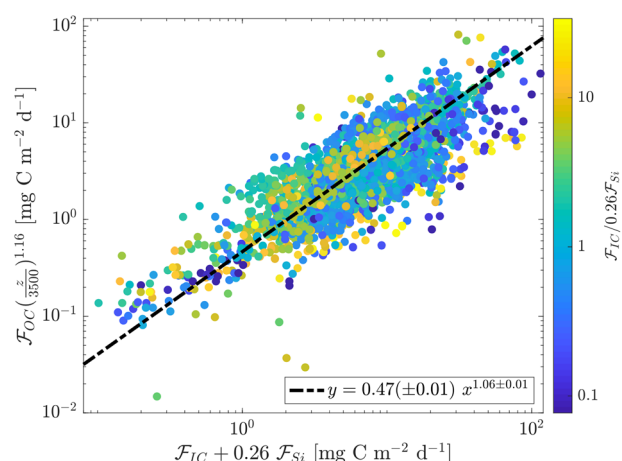
**Figure 3.** Scaling relationship predicting depth-normalized POC flux from a weighted sum of mineral fluxes. Color indicates ratio of calcium carbonate flux versus opal flux, weighted by $\beta$; dash-dotted black line is the inferred global scaling relationship $y = \kappa x^\gamma$. See Figure S3 for alternate version with smaller scatterpoints to show density of data. POC, particulate organic carbon.

Analogous scaling relationships are found for the four time-series that have measurements of both minerals alongside POC flux – ALOHA, CARIACO, K2, and OFP – though the depth-normalization parameter $b$ does not need to be estimated as each time-series' measurements are made at a single depth (Figure S4). CARIACO, K2, and OFP have similarly good fits ($r^2 = 0.81$, 0.88, and 0.84, respectively) and slightly sub-linear scaling relationships (i.e., non-linear with a scaling exponent lower than unity: $\gamma = 0.93 \pm 0.03$, $0.85 \pm 0.02$, and $0.92 \pm 0.02$, respectively), corresponding to a slightly systematically decreasing POC/mineral ratio with increasing mineral flux. Interestingly, CARIACO, K2, and OFP also have much larger $\beta$ values ($\beta = 1.45 \pm 0.33$, $1.84 \pm 0.40$, and $1.63 \pm 0.46$, respectively), indicating that per unit mass, opal has more organic carbon associated with it per unit mass in these locations. This underscores the important role that both minerals play, and that their relative importance can vary. The ALOHA time-series yields a much higher $\gamma = 1.40 \pm 0.11$ and $\beta = 15.6 \pm 10.9$, and a poorer fit ($r^2 = 0.47$). The large $\beta$ value further underscores the importance of opal flux depending on the time and place – it is known to be critical for deep export at Station ALOHA (Karl et al., 2012) – but also is highly unconstrained, so we caution against its overinterpretation. The spread in scaling exponents $\gamma$ between the time-series may be indicative of spatial variation in the mineral-POC flux dynamics around the global, approximately linear relationship; the global $\gamma = 1.06$ is close to the average (1.03) of the time-series' $\gamma$ values.

As the global $\beta$ we find is $0.26 \pm 0.01$, these findings suggest that perhaps aggregates containing, for example, diatom cells are ingested and remineralized more than, for example, aggregates containing coccolithophore cells and plates (liths). We cannot say from this work if these biominerals are truly ballasting POC because in some situations, these refractory biominerals may be all that remains after the labile POC is remineralized into the water column. Nonetheless, Figures 3 and S4 demonstrate that depth-normalized POC flux does scale approximately linearly with a weighted sum of these minerals; the scaling relationship is also quite strong given the variability in location and depth considered, and also appears to hold similarly for individual locations, though the relative weights of calcium carbonate versus opal differ between the global case and the local cases.

## 5. Dampening

We find an interesting consistency in the relationship between variability in NPP and variability in deep-sea flux, globally and across time-series, which is also consistent with the NPP-shallow flux relationship found in Cael et al. (2018). We estimate the log-standard deviation $\sigma$ of NPP at each site in the same manner as above and as in Cael et al. (2018), using $^{14}$C measurements taken as a part of the Hawai'i Ocean Time-series (HOT; Karl & Lukas, 1996), CARIACO time-series, and Bermuda Atlantic Time-series Study (BATS; Lomas et al., 2013; Steinberg et al., 2001) respectively for those locations, and all of the measurements in the data set used in Buitenhuis et al. (2013) and Cael et al. (2018) within 5° of the PAP and M sites for those locations; global $\sigma$ for NPP ($\sigma_{NPP}$) is taken from Cael et al. (2018) (Footnote 11 in the supporting information). As in Cael et al. (2018), we take the statistics of $^{14}$C measurements (Footnote 12 in the supporting information) to be reflective of the statistics of NPP, noting that all of the measurements used herein are subject to caveats, ambiguities, and uncertainties. We then compare the $\sigma$ for deep-sea POC flux ($\sigma_{\mathcal{F}}$) with the corresponding $\sigma_{NPP}$ in Figure 4. In Cael et al. (2018) we showed that if shallow flux scales with NPP and both are log-normal, the scaling exponent should correspond to a constant ratio of $\alpha = \sigma_{\mathcal{F}} / \sigma_{NPP}$, and we found $\alpha \sim 0.65 \pm 0.14$. The same is true here for deep flux; we regress the deep flux data in Figure 4 using the model $\sigma_{\mathcal{F}} = \alpha \sigma_{NPP}$ and find $\alpha = 0.62 \pm 0.04$ ($r^2 = 0.89$), in excellent agreement with the previous value. This implies that deep flux scales similarly with NPP to shallow flux, which in turn implies deep flux scales roughly linearly with shallow flux. As $\alpha < 1$, this also implies that all of the processes that collectively transform NPP eventually into deep-sea flux tend to dampen the variability in NPP. Ecologically, this
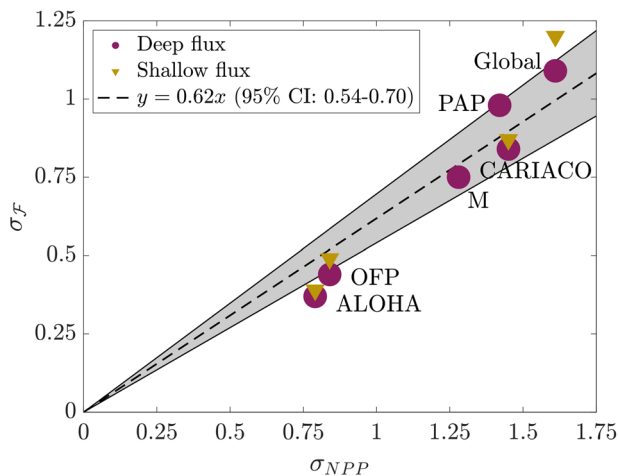
**Figure 4.** Log-standard deviation of net primary production versus deep-sea (purple) and shallow (yellow) organic carbon flux globally and for the time-series. Black line corresponds to $\sigma_{\mathcal{F}} / \sigma_{NPP} = 0.62$.

dampening effect could likely be caused by enhanced grazing, or heterotrophy in general, when NPP is high; if heterotrophs tend to consume a higher fraction of NPP when and where NPP is high, this would result in a negative correlation between $a \times ef$ (see §Global open ocean fluxes) and NPP, leading to $\sigma_{\mathcal{F}} < \sigma_{NPP}$ (Campbell, 1995). Such ecological dampening by the heterotrophic community would likely occur at shallower depths, that is, in the epipelagic and upper mesopelagic, where flux attenuation and organism abundances are highest (Iversen et al., 2010; Jackson & Checkley, 2011; van der Jagt et al., 2020). This is corroborated by the comparatively small differences between upper ocean export $\sigma$ values globally and for HOT, CARIACO, and BATS/OFP and their corresponding $\sigma_{\mathcal{F}}$ values (Cael et al., 2018; Figure 4), and the closeness of the $\alpha$ values derived from shallow and deep fluxes versus NPP. In Figure 4, $\sigma$ for shallow flux (flux measurements at ~150 m, a.k.a. export) is always between that of deep flux and NPP, but closer to that of deep flux, supporting the argument that most of the dampening of variability occurs at shallow depths. It has been argued that zooplankton act as gatekeepers for export flux at the base of the mixed layer (Jackson & Checkley, 2011); there is experimental evidence that zooplankton-phytoplankton dynamics follow such dampening patterns and that this dampens carbon export variability (van der Jagt et al., 2020) but this dampening has not been demonstrated on the global scale. Globally representative measurements similar to those made in van der Jagt et al. (2020) would be valuable for testing whether similar mechanisms underlie this variability dampening at the global scale. Because NPP and flux observations are taken over different space and timescales, however, it is not clear how much of these $\sigma$ differences can be attributed to ecological processes. The difference in measurement scales should reduce deep-sea $\sigma_{\mathcal{F}}$ relative to shallow $\sigma_{\mathcal{F}}$, and shallow $\sigma_{\mathcal{F}}$ relative to $\sigma_{NPP}$; regardless of this measurement-produced offset, however, the coherence in the differences between $\sigma$ values in Figure 4 does imply a consistent relationship between the variability in NPP and the variability in deep-sea POC flux across scales and locations.

## 6. Episodicity

Is the benthos supplied by episodic flux events or a steady rain of particles? This question can be assessed quantitatively in terms of how heavy the tail of the probability distribution of fluxes is. Log-normals are one of a class of "heavy-tailed" distributions for which values much larger than the mean are not uncommon, but are not as heavy-tailed as other probability distributions commonly found in nature, such as a power-law distribution. The degree of heavy-tailedness or episodicity can be quantified simply in terms of the joint ratio (Footnote 13 in the supporting information): The $(100 - X)/X$ such that $X\%$ of the largest values contribute $(100 - X)\%$ of the sum of all the values. For the global $\mathcal{F}_{OC}$ data, both the observations and the log-normal fit yield a joint ratio of 71/29, corresponding to an imbalanced distribution, but a less imbalanced one than the classical 80/20 "Pareto principle" benchmark of a heavily imbalanced distribution in social, economic, and other natural systems (Sanders, 1987). This also holds for minerals and for time-series; all of the global distributions' joint ratios were between 70/30 and 75/25, and all of the time-series' distributions' joint ratios were between 60/40 and 75/25 (Footnote 14 in the supporting information). This implies an intermediate answer to the episodicity question; the deep-sea flux distributions are heavy-tailed enough that high-flux pulses do play an important role in supplying the benthos, but not heavy-tailed enough that such pulses dominate total supply. This measure of episodicity is however only in terms of the (~weekly or longer) time intervals over which these deep flux measurements are taken. There will be variations in flux during these time intervals and so the true flux will be more episodic than the calculated episodicity from these time-averaged values. Furthermore, other relevant supplies to the benthos, such as energy (Grabowski et al., 2019) or genes linked to particular substrates (Boeuf et al., 2019), appear to be more episodic than organic carbon; the composition, nature and value of the supplied material may therefore be more episodic as well. Finally, these global and time-series data are heavily representative of temperate and subtropi-

cal systems. Polar or shelf systems are known to be extremely episodic, sometimes with total export/supply dominated by a single regular seasonal event (e.g., Amiel and Cochran (2008), Ducklow et al. (2015), and references therein). We thus expect different degrees of episodicity in these systems, and potentially non-log-normally distributed fluxes.

## 7. Discussion

It is important to recognize that while the propagation of log-normality from NPP, to export out of the upper ocean, to deep-sea flux is intuitive when cast in terms of an export efficiency and an attenuation factor; in reality particle fluxes are very complicated and that this over-simplification appears to work so well is rather surprising. Deep-sea traps integrate over large spatial areas (Siegel & Deuser, 1997) that can be strongly influenced by lateral advection and stirring. Productivity and even export can vary greatly on much smaller scales (Estapa et al., 2015; Mahadevan, 2016). Particles sinking with a wide range of settling velocities contribute appreciably to total flux (Trull et al., 2008) meaning a deep-sea flux measurement is also a convolution of productivity at different times; deep-sea particle fluxes are also measured on timescales of weeks, unlike those of NPP or upper ocean export, which are measured on timescales of a day or days, respectively. NPP occurs throughout the euphotic layer and its depth-dependence varies (Behrenfeld & Falkowski, 1997). All of these factors complicate any one-to-one relationship between the value of a NPP measurement and the value of a corresponding deep-sea flux measurement. Nonetheless, our results indicate that these complications do not prevent log-normality from propagating into deep-sea fluxes. We also note that the log-normal description is agnostic as to the driver(s) of these fluxes and their variations.

To conclude, we have shown that the log-normality of NPP measurements propagates from upper-ocean fluxes through the water column to near-seafloor fluxes, both globally and for individual time-series, both for organic carbon and for opal and calcium carbonate. This provides a simple way to characterize the variability of these fluxes, the organic carbon associations of these minerals, and the link between NPP and deep-sea flux on large scales. The issue of spatial and temporal measurement scale is an important one to address in future work, and will make it possible to capitalize on these distributional relationships, for example, to link satellite models of NPP with upper-ocean and even deep-sea carbon fluxes.

## Data Availability Statement

OFP data are available from the NSF Biological and Chemical Oceanography Data Management Office (BCO-DMO). Data and code are available at https://doi.org/10.5281/zenodo.4675075. For review, the global data can be found from the Cael et al. (2018) and Mouw et al. (2016) sources cited in the text, and the time-series data can be found at https://github.com/bbcael/grl-deep-flux-preliminary-data.

## References

Amiel, D., & Cochran, J. K. (2008). Terrestrial and marine POC fluxes derived from $^{234}$Th distributions and $\delta^{13}$C measurements on the Mackenzie Shelf. *Journal of Geophysical Research*, *113*(C3). https://doi.org/10.1029/2007jc004260

Armstrong, R. A., Lee, C., Hedges, J. I., Honjo, S., & Wakeham, S. G. (2001). A new, mechanistic model for organic carbon fluxes in the ocean based on the quantitative association of POC with ballast minerals. *Deep Sea Research Part II: Topical Studies in Oceanography*, *49*(1–3), 219–236. https://doi.org/10.1016/s0967-0645(01)00101-1

Behrenfeld, M. J., & Falkowski, P. G. (1997). A consumer's guide to phytoplankton primary productivity models. *Limnology & Oceanography*, *42*(7), 1479–1491. https://doi.org/10.4319/lo.1997.42.7.1479

Bisson, K. M., Siegel, D. A., DeVries, T., Cael, B. B., & Buesseler, K. O. (2018). How data set characteristics influence ocean carbon export models. *Global Biogeochemical Cycles*, *32*(9), 1312–1328. https://doi.org/10.1029/2018gb005934

Boeuf, D., Edwards, B. R., Eppley, J. M., Hu, S. K., Poff, K. E., Romano, A. E., et al. (2019). Biological composition and microbial dynamics of sinking particulate organic matter at abyssal depths in the oligotrophic open ocean. *Proceedings of the National Academy of Sciences*, *116*(24), 11824–11832.

Boyd, P. W., Claustre, H., Levy, M., Siegel, D. A., & Weber, T. (2019). Multi-faceted particle pumps drive carbon sequestration in the ocean. *Nature*, *568*(7752), 327–335. https://doi.org/10.1038/s41586-019-1098-2

Boyd, P. W., & Trull, T. W. (2007). Understanding the export of biogenic particles in oceanic waters: Is there consensus? *Progress in Oceanography*, *72*(4), 276–312. https://doi.org/10.1016/j.pocean.2006.10.007

Buesseler, K. O. (1998). The decoupling of production and particulate export in the surface ocean. *Global Biogeochemical Cycles*, *12*(2), 297–310. https://doi.org/10.1029/97gb03366

Buesseler, K. O., Antia, A. N., Chen, M., Fowler, S. W., Gardner, W. D., Gustafsson, O., et al. (2007). An assessment of the use of sediment traps for estimating upper ocean particle fluxes. *Journal of Marine Research*, *65*(3), 345–416. https://doi.org/10.1357/002224007781567621

Buesseler, K. O., & Boyd, P. W. (2009). Shedding light on processes that control particle export and flux attenuation in the twilight zone of the open ocean. *Limnology & Oceanography*, *54*(4), 1210–1232. https://doi.org/10.4319/lo.2009.54.4.1210

Buesseler, K. O., Steinberg, D. K., Michaels, A. F., Johnson, R. J., Andrews, J. E., Valdes, J. R., & Price, J. F. (2000). A comparison of the quantity and composition of material caught in a neutrally buoyant versus surface-tethered sediment trap. *Deep Sea Research Part I: Oceanographic Research Papers*, *47*(2), 277–294. https://doi.org/10.1016/s0967-0637(99)00056-4

Buitenhuis, E. T., Hashioka, T., & Quéré, C. L. (2013). Combined constraints on global ocean primary production using observations and models. *Global Biogeochemical Cycles*, *27*(3), 847–858. https://doi.org/10.1002/gbc.20074

Cael, B. B., & Bisson, K. (2018). Particle flux parameterizations: Quantitative and mechanistic similarities and differences. *Frontiers in Marine Science*, *5*, 395. https://doi.org/10.3389/fmars.2018.00395

Cael, B. B., Bisson, K., & Follett, C. L. (2018). Can rates of ocean primary production and biological carbon export be related through their probability distributions? *Global Biogeochemical Cycles*, *32*(6), 954–970. https://doi.org/10.1029/2017gb005797

Cael, B. B., & Follows, M. J. (2016). On the temperature dependence of oceanic export efficiency. *Geophysical Research Letters*, *43*(10), 5170–5175. https://doi.org/10.1002/2016gl068877

Campbell, J. W. (1995). The lognormal distribution as a model for bio-optical variability in the sea. *Journal of Geophysical Research*, *100*(C7), 13237–13254. https://doi.org/10.1029/95jc00458

Conte, M. H., Carter, A. M., Koweek, D. A., Huang, S., & Weber, J. C. (2019). The elemental composition of the deep particle flux in the Sargasso Sea. *Chemical Geology*, *511*, 279–313. https://doi.org/10.1016/j.chemgeo.2018.11.001

Conte, M. H., Dickey, T., Weber, J., Johnson, R., & Knap, A. (2003). Transient physical forcing of pulsed export of bioreactive material to the deep Sargasso Sea. *Deep Sea Research Part I: Oceanographic Research Papers*, *50*(10–11), 1157–1187. https://doi.org/10.1016/s0967-0637(03)00141-9

Conte, M. H., Ralph, N., & Ross, E. H. (2001). Seasonal and interannual variability in deep ocean particle fluxes at the Oceanic Flux Program (OFP)/Bermuda Atlantic Time Series (BATS) site in the western Sargasso Sea near Bermuda. *Deep Sea Research Part II: Topical Studies in Oceanography*, *48*(8–9), 1471–1505. https://doi.org/10.1016/s0967-0645(00)00150-8

Conte, M. H., & Weber, J. (2014). Particle flux in the deep Sargasso Sea: The 35-year oceanic flux program time series. *Oceanography*, *27*(1), 142–147. https://doi.org/10.5670/oceanog.2014.17

Ducklow, H. W., Wilson, S. E., Post, A. F., Stammerjohn, S. E., Erickson, M., Lee, S., et al. (2015). Particle flux on the continental shelf in the Amundsen Sea Polynya and Western Antarctic Peninsula. *Elementa: Science of the Anthropocene*, *3*. https://doi.org/10.12952/journal.elementa.000046

Eppley, R. W., & Peterson, B. J. (1979). Particulate organic matter flux and planktonic new production in the deep ocean. *Nature*, *282*(5740), 677–680. https://doi.org/10.1038/282677a0

Estapa, M. L., Siegel, D. A., Buesseler, K. O., Stanley, R. H. R., Lomas, M. W., & Nelson, N. B. (2015). Decoupling of net community and export production on submesoscales in the Sargasso Sea. *Global Biogeochemical Cycles*, *29*(8), 1266–1282. https://doi.org/10.1002/2014gb004913

Follett, C. L., Dutkiewicz, S., Karl, D. M., Inomura, K., & Follows, M. J. (2018). Seasonal resource conditions favor a summertime increase in North Pacific diatom-diazotroph associations. *The ISME Journal*, *12*(6), 1543–1557. https://doi.org/10.1038/s41396-017-0012-x

Francois, R., Honjo, S., Krishfield, R., & Manganini, S. (2002). Factors controlling the flux of organic carbon to the bathypelagic zone of the ocean. *Global Biogeochemical Cycles*, *16*(4), 34-1–34-20. https://doi.org/10.1029/2001gb001722

Grabowski, E., Letelier, R. M., Laws, E. A., & Karl, D. M. (2019). Coupling carbon and energy fluxes in the North Pacific Subtropical Gyre. *Nature Communications*, *10*(1), 1–9. https://doi.org/10.1038/s41467-019-09772-z

Henson, S. A., Sanders, R., & Madsen, E. (2012). Global patterns in efficiency of particulate organic carbon export and transfer to the deep ocean. *Global Biogeochemical Cycles*, *26*(1). https://doi.org/10.1029/2011gb004099

Henson, S. A., Sanders, R., Madsen, E., Morris, P. J., Le Moigne, F., & Quartly, G. D. (2011). A reduced estimate of the strength of the ocean's biological carbon pump. *Geophysical Research Letters*, *38*(4). https://doi.org/10.1029/2011gl046735

Honda, M. C. (2020). Effective vertical transport of particulate organic carbon in the western North Pacific Subarctic region. *Frontiers of Earth Science*, *8*, 366. https://doi.org/10.3389/feart.2020.00366

Ito, T., & Follows, M. J. (2005). Preformed phosphate, soft tissue pump and atmospheric $CO_2$. *Journal of Marine Research*, *63*(4), 813–839. https://doi.org/10.1357/0022240054663231

Iversen, M. H., Nowald, N., Ploug, H., Jackson, G. A., & Fischer, G. (2010). High resolution profiles of vertical particulate organic matter export off Cape Blanc, Mauritania: Degradation processes and ballasting effects. *Deep Sea Research Part I: Oceanographic Research Papers*, *57*(6), 771–784. https://doi.org/10.1016/j.dsr.2010.03.007

Jackson, G. A., & Checkley, D. M., Jr. (2011). Particle size distributions in the upper 100 m water column and their implications for animal feeding in the plankton. *Deep Sea Research Part I: Oceanographic Research Papers*, *58*(3), 283–297. https://doi.org/10.1016/j.dsr.2010.12.008

Karl, D. M., Church, M. J., Dore, J. E., Letelier, R. M., & Mahaffey, C. (2012). Predictable and efficient carbon sequestration in the North Pacific Ocean supported by symbiotic nitrogen fixation. *Proceedings of the National Academy of Sciences*, *109*(6), 1842–1849. https://doi.org/10.1073/pnas.1120312109

Karl, D. M., & Lukas, R. (1996). The Hawaii Ocean Time-series (HOT) program: Background, rationale and field implementation. *Deep Sea Research Part II: Topical Studies in Oceanography*, *43*(2–3), 129–156. https://doi.org/10.1016/0967-0645(96)00005-7

Klaas, C., & Archer, D. E. (2002). Association of sinking organic matter with various types of mineral ballast in the deep sea: Implications for the rain ratio. *Global Biogeochemical Cycles*, *16*(4), 63-1–63-14. https://doi.org/10.1029/2001gb001765

Lam, P. J., & Bishop, J. K. (2008). The continental margin is a key source of iron to the HNLC North Pacific Ocean. *Geophysical Research Letters*, *35*(7). https://doi.org/10.1029/2008gl033294

Lampitt, R. S., Billett, D. S. M., & Martin, A. P. (2010). The sustained observatory over the Porcupine Abyssal Plain (PAP): Insights from time series observations and process studies. *Deep Sea Research Part II: Topical Studies in Oceanography*, *57*(15), 1267–1271. https://doi.org/10.1016/j.dsr2.2010.01.003

Letelier, R. M., Björkman, K. M., Church, M. J., Hamilton, D. S., Mahowald, N. M., Scanza, R. A., et al. (2019). Climate-driven oscillation of phosphorus and iron limitation in the North Pacific Subtropical Gyre. *Proceedings of the National Academy of Sciences*, *116*(26), 12720–12728. https://doi.org/10.1073/pnas.1900789116

Limpert, E., Stahel, W. A., & Abbt, M. (2001). Log-normal distributions across the sciences: Keys and clues. *BioScience*, *51*(5), 341–352. https://doi.org/10.1641/0006-3568(2001)051[0341:lndats]2.0.co;2

Lomas, M. W., Bates, N. R., Johnson, R. J., Knap, A. H., Steinberg, D. K., & Carlson, C. A. (2013). Two decades and counting: 24-years of sustained open ocean biogeochemical measurements in the Sargasso Sea. *Deep Sea Research Part II: Topical Studies in Oceanography*, *93*, 16–32. https://doi.org/10.1016/j.dsr2.2013.01.008

Mahadevan, A. (2016). The impact of submesoscale physics on primary productivity of plankton. *Annual Review of Marine Science*, *8*, 161–184. https://doi.org/10.1146/annurev-marine-010814-015912

Martin, J. H., Knauer, G. A., Karl, D. M., & Broenkow, W. W. (1987). VERTEX: Carbon cycling in the northeast Pacific. *Deep-Sea Research Part A. Oceanographic Research Papers*, *34*(2), 267–285. https://doi.org/10.1016/0198-0149(87)90086-0

Mouw, C. B., Barnett, A., McKinley, G. A., Gloege, L., & Pilcher, D. (2016). Global ocean particulate organic carbon flux merged with satellite parameters. *Earth System Science Data*, *8*, 531–541. https://doi.org/10.5194/essd-8-531-2016

Muller-Karger, F. E., Astor, Y. M., Benitez-Nelson, C. R., Buck, K. N., Fanning, K. A., Lorenzoni, L., et al. (2019). The scientific legacy of the CARIACO ocean time-series program. *Annual Review of Marine Science*, *11*, 413–437. https://doi.org/10.1146/annurev-marine-010318-095150

Muller-Karger, F. E., Varela, R., Thunell, R., Luerssen, R., Hu, C., & Walsh, J. J. (2005). The importance of continental margins in the global carbon cycle. *Geophysical Research Letters*, *32*(1). https://doi.org/10.1029/2004gl021346

Olli, K. (2015). Unraveling the uncertainty and error propagation in the vertical flux Martin curve. *Progress in Oceanography*, *135*, 146–155. https://doi.org/10.1016/j.pocean.2015.05.016

Osmond, C. B. (1989). Photosynthesis from the molecule to the biosphere: A challenge for integration. In W. R. Briggs (Ed.), *Photosynthesis* (pp. 5–17). Alan R. Liss Inc.

Passow, U., & De La Rocha, C. L. (2006). Accumulation of mineral ballast on organic aggregates. *Global Biogeochemical Cycles*, *20*(1). https://doi.org/10.1029/2005gb002579

Plattner, G.-K., Gruber, N., Frenzel, H., & McWilliams, J. C. (2005). Decoupling marine export production from new production. *Geophysical Research Letters*, *32*(11). https://doi.org/10.1029/2005gl022660

Rokop, F. J. (1974). Reproductive patterns in the deep-sea benthos. *Science*, *186*(4165), 743–745. https://doi.org/10.1126/science.186.4165.743

Ruhl, R. H. R., Buesseler, K. O., Manganini, S. J., Steinberg, D. K., & Valdes, J. R. (2004). A comparison of major and minor elemental fluxes collected in neutrally buoyant and surface-tethered sediment traps. *Deep Sea Research Part I: Oceanographic Research Papers*, *51*(10), 1387–1395. https://doi.org/10.1016/j.dsr.2004.05.010

Sanders, R. (1987). The Pareto principle: Its use and abuse. *Journal of Services Marketing*, *1*(2), 37–40. https://doi.org/10.1108/eb024706

Siegel, D., & Deuser, W. (1997). Trajectories of sinking particles in the Sargasso Sea: Modeling of statistical funnels above deep-ocean sediment traps. *Deep Sea Research Part I: Oceanographic Research Papers*, *44*(9–10), 1519–1541. https://doi.org/10.1016/s0967-0637(97)00028-9

Smith, K. L. J., Jr., Sherman, A. D., Huffard, C. L., McGill, P. R., Henthorn, R., Von Thun, S., et al. (2014). Large salp bloom export from the upper ocean and benthic community response in the abyssal northeast Pacific: Day to week resolution. *Limnology & Oceanography*, *59*(3), 745–757. https://doi.org/10.4319/lo.2014.59.3.0745

Smith, K. L., Jr., Ruhl, H. A., Huffard, C. L., Messié, M., & Kahru, M. (2018). Episodic organic carbon fluxes from surface ocean to abyssal depths during long-term monitoring in NE Pacific. *Proceedings of the National Academy of Sciences*, *115*(48), 12235–12240. https://doi.org/10.1073/pnas.1814559115

Steinberg, D. K., Carlson, C. A., Bates, N. R., Johnson, R. J., Michaels, A. F., & Knap, A. H. (2001). Overview of the US JGOFS Bermuda Atlantic Time-series Study (BATS): A decade-scale look at ocean biology and biogeochemistry. *Deep Sea Research Part II: Topical Studies in Oceanography*, *48*(8–9), 1405–1447. https://doi.org/10.1016/s0967-0645(00)00148-x

Stephens, M. A. (1974). EDF statistics for goodness of fit and some comparisons. *Journal of the American Statistical Association*, *69*(347), 730–737. https://doi.org/10.1080/01621459.1974.10480196

Suess, E. (1980). Particulate organic carbon flux in the oceans-surface productivity and oxygen utilization. *Nature*, *288*(5788), 260–263. https://doi.org/10.1038/288260a0

Trull, T., Bray, S., Buesseler, K., Lamborg, C., Manganini, S., Moy, C., & Valdes, J. (2008). In situ measurement of mesopelagic particle sinking rates and the control of carbon transfer to the ocean interior during the Vertical Flux in the Global Ocean (VERTIGO) voyages in the North Pacific. *Deep Sea Research Part II: Topical Studies in Oceanography*, *55*(14–15), 1684–1695. https://doi.org/10.1016/j.dsr2.2008.04.021

van der Jagt, H., Wiedmann, I., Hildebrandt, N., Niehoff, B., & Iversen, M. H. (2020). Aggregate feeding by the copepods *Calanus and Pseudocalanus* controls carbon flux attenuation in the Arctic shelf sea during the productive period. *Frontiers in Marine Science*, *7*, 543124. https://doi.org/10.3389/fmars.2020.543124

Wiedmann, I., Ceballos-Romero, E., Villa-Alfageme, M., Renner, A., Dybwad, C., van der Jagt, H., et al. (2020). Arctic observations identify phytoplankton community composition as driver of carbon flux attenuation. *Geophysical Research Letters*, *47*(14), e2020GL087465. https://doi.org/10.1029/2020gl087465

## References From the Supporting Information

Gloege, L., McKinley, G. A., Mouw, C. B., & Ciochetto, A. B. (2017). Global evaluation of particulate organic carbon flux parameterizations and implications for atmospheric pCO$_2$. *Global Biogeochemical Cycles*, *31*(7), 1192–1215. https://doi.org/10.1002/2016gb005535

Lampitt, R. S., & Antia, A. N. (1997). Particle flux in deep seas: Regional characteristics and temporal variability. *Deep Sea Research Part I: Oceanographic Research Papers*, *44*(8), 1377–1403. https://doi.org/10.1016/s0967-0637(97)00020-4

Marra, J. (2009). Net and gross productivity: Weighing in with $^{14}$C. *Aquatic Microbial Ecology*, *56*(2–3), 123–131. https://doi.org/10.3354/ame01306

Pei, S., & Laws, E. A. (2013). Does the $^{14}$C method estimate net photosynthesis? Implications from batch and continuous culture studies of marine phytoplankton. *Deep Sea Research Part I: Oceanographic Research Papers*, *82*, 1–9. https://doi.org/10.1016/j.dsr.2013.07.011

Peterson, B. J. (1980). Aquatic primary productivity and the $^{14}$C-CO$_2$ method: A history of the productivity problem. *Annual Review of Ecology and Systematics*, *11*(1), 359–385. https://doi.org/10.1146/annurev.es.11.110180.002043